J Intell Robot Syst (2017) 85:189–206
DOI 10.1007/s10846-016-0382-8

Toward Optimal Rendezvous of Multiple Underwater Gliders: 3D Path Planning with Combined Sawtooth and Spiral Motion

Junliang Cao · Junjun Cao · Zheng Zeng · Baoheng Yao · Lian Lian

Received: 30 April 2015 / Accepted: 22 May 2016 / Published online: 8 June 2016

Abstract In this paper, a path planning system is proposed for optimal rendezvous of multiple underwater gliders in three-dimensional (3D) space. Inspired by the Dubins Paths consisting of straight lines and circular arcs, this paper presents the first attempt to extend the 3D Dubins curve to accommodate the characteristic glider motions include upwards and downwards straight glides in a sawtooth pattern and gliding in a vertical spiral. This modified 3D Dubins scheme is combined with genetic algorithm (GA), together with a rendezvous position selection scheme to find rendezvous trajectories for multiple gliders with minimal energy consumption over all participating vehicles. The properties and capabilities of the proposed path planning methodology are illustrated for several rendezvous mission scenarios. First, a simple application was performed for a single glider to rendezvous with a fix dock. Simulation results show the proposed planner is able to obtain more optimized trajectories when compared with the typical Dubins trajectory with nominal velocity. Additional representative simulations were run to analyse the performance of this path planner for multiple gliders rendezvous. The results demonstrate that the proposed path planner identifies the optimal rendezvous location and generates the corresponding rendezvous trajectories for multiple gliders that ensures they reach their destination with optimized energy consumption.

Keywords Path planning · 3D Dubins path · Energy consumption · Rendezvous planning · Multiple underwater gliders

J. Cao · J. Cao · Z. Zeng (✉) · B. Yao · L. Lian (✉)
State Key Laboratory of Ocean Engineering, Shanghai Jiao Tong University, Shanghai 200240, China
e-mail: zheng.zeng@sjtu.edu.cn
e-mail: llian@sjtu.edu.cn

Z. Zeng · B. Yao · L. Lian
Institute of Oceanology, Shanghai Jiao Tong University, Shanghai 200240, China

Z. Zeng · B. Yao · L. Lian
Qingdao Collaborative Innovation Center of Marine Science and Technology, Qingdao, China

1 Introduction

Marine scientists have envisioned the use of autonomous underwater vehicles (AUVs) for oceanographic monitoring. However, long-range and long-duration deployments are limited by the propulsion system of conventional AUVs. Buoyancy driven underwater gliders, are highly efficient winged underwater vehicles driven by modifying the net buoyancy and internal shape. In a quintessential configuration, a buoyancy bladder modulates the glider's netbuoyancy while a movable and rotatable mass actuator modulates its center of gravity (CG) relative to the

center of buoyancy (CB). Underwater gliders are characterized with low energy consumption, low cost, and long range, such as the commercially available gliders Slocum [1, 2], Spray [3], and Seaglider [4]. For decades, as novel and efficient underwater vehicles for ocean exploring and prospecting, underwater gliders have been widely applied to ocean research.

Multiple cooperative underwater gliders system holds great promise for use in large scale oceanographic surveys, mine counter-measurement missions and other similar offshore tasks due to better resource and task allocation [5]. Simultaneous use of multiple vehicles, including complementary use of differently-capable underwater gliders or combined operation of surface vehicles and underwater gliders, can improve performance, reduce mission time, provide broader or more robust data, and increase the likelihood of mission success. Rendezvous at a specified location is one of the missions for multiple cooperative vehicle systems [6]. The purpose of rendezvous could be an initial step in formation creation, data exchange, vehicle recharging, maintenance, or collection [7]. A conceptually scenario could be, at the completion of the mission, the glider surfaces and rendezvous with the platforms such as marine vehicles and moorings for recovery. The literature on this topic has been dominated by single vehicle planning [8, 9], considerable work has still to be done to develop advanced methods for cooperative path planning for multiple gliders that explicitly address the problem of rendezvous.

Path planning for rendezvous concept should be optimized in order to satisfy the objectives of the operation. One objective of the rendezvous idea is to accelerate accessing of data collected by the underwater gliders, it may be desirable to plan trajectories for underwater glider such that it can complete rendezvous as fast as possible [10, 11]. Recognizing the energy limitations of underwater gliders, another main objective is instead to perform each rendezvous using the minimal possible energy [12, 13]. These energy-optimal solutions reserve maximal energy for glider fleet to exchange data after rendezvous. Other optimization objectives may also be desirable. This work addresses planning optimal trajectories that consumes minimal amount of energy for multiple underwater gliders to achieve the rendezvous destination.

A variety of approaches have been developed and applied to the path planning problem for underwater vehicle (for details, see Section 2). Although a large number of methods have been proposed, there is still considerable work to be done to develop advanced methods for glider-oriented applications. Conventional path planning approaches project the 3D environment to two-dimensional (2D) space. However, this 2D trajectory cannot embody complete 3D information of the trajectory which is essential for rendezvous purpose. Toward planning rendezvous trajectories for underwater gliders, this work expands upon the typical 2D Dubins Paths consisting of straight lines and circular arcs, presents a novel 3D Dubins curve which is able to accommodate the characteristic glider motions include upwards and downwards straight glides in a sawtooth pattern and gliding in a vertical spiral.

Another main limitation of the state of the art approaches for underwater glider path planning is that they assume the final heading angle is deterministic selected [14]. Indeed the destination position is fixed in advance, which is necessary to evaluate the travel cost of the vehicle. However, in many applications, the final heading angle can be flexible. In such situations, the choice of an appropriate final heading angle is a critical issue. It should avoid the vehicle arrive at the destination but making a big turn to match the final heading angle.

In this study, the extended 3D Dubins curve is developed and integrated into the GA-based path planner. The proposed path planner builds upon the steady state solutions of motion and thorough energy consumption analysis of the glider system. It is also combined with a novel rendezvous position selection scheme to find optimal trajectory along with identified motion configuration (velocity, turning radius, and path angle), heading, and destination that ensures the glider travels with minimal energy consumption. Builds upon the 3D path planning solutions developed for a single glider rendezvous with a fix dock, a complete and detailed description of rendezvous path planning scheme for multiple underwater gliders is presented in this paper. Moreove, the performance analyses for the path planner as well as statistical assessment of performance with various scenarios is presented.

The rest of this paper is organized as follows. The problem to be solved in this study is formulated in Section 3, including the 3D Dubins path problem for an underwater glider, the steady state solution of dynamic equilibrium, and the energy consumption

analysis in the glider system. Section 4 outlines the system structure of the proposed GA-based path planner. The simulation studies of single and multiple gliders under various scenarios are presented in Section 5. The conclusions and future works are then discussed in Section 6.

2 Related Work

In this section, it is introduced how our work is related to the vast body of work on planning for robots that is already present in the literature. Optimization techniques for robots path planning is a well-studied problem [15]. A variety of approaches have been developed and applied to the path planning problem for underwater vehicles. These include Dijkstra's algorithm [16], A* algorithm [17], Field D* algorithm [18], Fast Marching (FM) algorithm [19], Artificial Potential Field [20], and rapidly exploring random tree (RRT) [21]. A brief comparison of these path planning techniques for underwater vehicles with discussion of their assumptions and drawbacks is available in [22]. Evolutionary algorithms are also applied for generating the optimal trajectory. GA [23, 24] and the particle swarm optimization (PSO) [25, 26] are two well-known forms of evolutionary algorithms that are generally recognized to be effective optimization techniques for solving path planning problems. Their computational cost grows linearly with the number of vehicles and geometrically with spatial dimensions. Also, GA has the advance performance over PSO to escape from local minima. Recently, Zheng [22] applied the imperialist competitive algorithm (ICA) for path planning and showed that it has superior performance compared to the standard PSO and GA algorithms. However, ICA is sensitive to the tuning of its parameters and research is still in progress to reduce this sensitivity.

The shape and properties of the path have a direct influence on the path planning system. In many early applications, the path is defined as the sum of the successive straight lines that connect these waypoints. Due to physical constraints of underwater gliders though, it is not possible for a vehicle to achieve a smooth transition between two straight lines because such a path generally has a discontinuous first derivative at the locations of the waypoints. Viewing the glider motion from directly above, the minimum time control problem is reminiscent of Dubins path [27, 28], a planar vehicle which drives forward at constant speed and which may turn, in either direction, at any rate up to some maximum value. Variations of Dubins problem have enjoyed renewed attention in recent years, in part because of increasing interest in mobile robotics [29, 30]. Techy and Woolsey [31], deal with the problem of finding a Dubins path for a vehicle that moves in a constant drifted (can be wind or current for aerial or marine vehicles, respectively). The 3D Dubins path problem for an Unmanned Aerial Vehicle (UAV) is an attractive study in recent years [32–34]. Zhu et al. [35, 36] extended the Dubins problem to underwater space, multi-AUVs are formed into group to search for a target. However, the Dubins problem of an underwater glider is distinctive from other vehicles due to its particular ways of motion. Most of the existing work is done by Mahmoudian et al. [37, 38]: the minimal time path is established where only turn radius is considered, meanwhile the horizontal and vertical components of velocity remain constant. The minimal time path is compared with the suboptimal path [39] in the horizontal plane based on the approximate solution to steady turning.

3 Problem Definition

This research focus on the recovery of underwater glider and efficient interception with other marine platforms. Specifically, a path planner is proposed to generate the trajectories for underwater gliders that lead to the energy-efficient pick up by an unmanned surface vehicle (USV), or intercept with platforms such as AUVs/gliders (mobile) and moorings (stationary). Figure 1 depicts a conceptually simple scenario where, at the completion of the mission, the glider surfaces and rendezvous with the USV for recovery. Gliders are commonly equipped with a GPS and Iridium Satellite communication, after surfacing, the glider transmits data regarding its profile, position and status via satellite to the USV. The path planner on the USV then determines the trajectories on-line based on this information received from the glider. These trajectories should allow the glider and USV to arrive at their rendezvous point with minimum energy cost. It is only after the glider receives the trajectory profile from the USV that the glider can dive down and accomplishes the rendezvous.

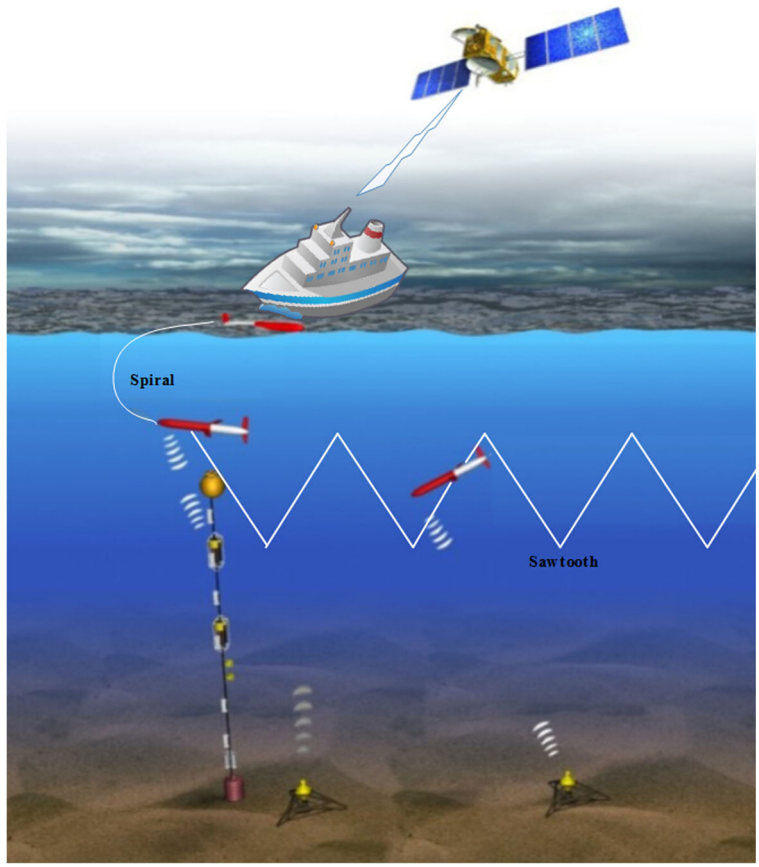

Fig. 1 3D path planning with combined sawtooth and spiral motion

The path planner in this work aims to reduce the energy consumption of the gliders in the rendezvous process using a GA-based path planner described in Section 4. In this section, we will begin with a description of the problem, which aims at minimizing the energy consumption for multiple gliders to complete the rendezvous mission with considering the characteristic glider motions. Next, we briefly describe the modified 3D Dubins curve we use to accommodate the combined sawtooth and spiral glider motions. Finally, we introduce an approximate semi-analytical solution to compute the steady state inputs of the spiral motionbefore providing a calculation of the energy consumption we use throughout our paper.

3.1 Problem Formulation

Define the minimum energy consumption path $P^* = [s_0, ..., s_f]$ as the optimal path among all feasible paths $\mathcal{P}$, going from s_0 to s_f, where s_0 is the initial condition and s_f is the final condition,

$$P^* = \min_{P \in \mathcal{P}} \sum_{i=1}^{|P|} energy(s_i) \tag{1}$$

where $s_i = (x_i, y_i)^T$ is a waypoint along the path $P = [s_0, ..., s_f]$ and $energy(s_i)$ is the value of energy consumption at node s_i.

The measurement of energy consumption varies with the mechanical actuators inside the vehicle system,

$$energy(s_i) = \sum_{j=1} e_r(u_j) \tag{2}$$

where u_j is the control input of the atuator, and $e_r(u_j)$ is the rate of energy consumption of each actuator. For

an underwater glider, the mechanical acturtors usually include the buoyancy engine, the linear actuator, the rotational actuator, and the electronic system; the details will be thoroughly analyzed in Section 3.4.

A reasonable way to determine the control inputs is to solve the equations of motions, including both sawtooth and spiral motion, at equilibrium state. The motion configurations: turning radius (R), velocity (V), and gliding path angle (ξ) are fundamentals to describe a trajectory, the solution to this problem (Eq. 3) will be introduced in Section 3.3.

$$(u_1, ..., u_j) = equilibrium(R, V, \xi) \tag{3}$$

Besides the motion configurations for a single glider, more characteristics should be considered in the situation of rendezvous problem for multiple underwater gliders, such as the common final heading and final destination.

3.2 Modified 3D Dubins for Combined Sawtooth and Spiral Motion

As mentioned before, the 3D motion is distinguished from an UAV or AUV due to the particular diving mode. The poor maneuvering performance makes underwater glider operate in a certain angle in the motion, and the turning radius is limited to a specified value. Besides, the operating depth is also restricted due to the tremendous pressure in the deep water environment. Therefore, the 3D Dubins path of an underwater glider is consisted of n full-depth diving cycles ($n \geqslant 0$) and one final regulating period, as shown in Fig. 2.

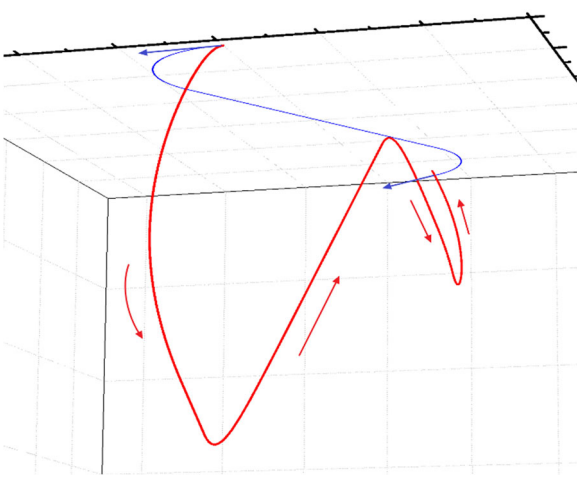

Fig. 2 Example of 3D-Dubins path for an underwater glider (RSL)

According to Boissonnat et al. [40], with given configurations, the optimal Dubins path exists among six types, which can be divided into two families. The first family starts with a left (L) or right (R) turning, follows by a straight segment (S), and ends up with a left or right turning (denoted by LSR, LSL, RSL, and RSR, respectively). In the other family, an arc of circle can be followed with opposite directions instead of the straight segment (denoted by RLR and LRL) under certain circumstances.

The existence of each situation is based on the initial conditions, varies from 4 to 6 types accordingly. Establishing the earth-frame at the initial point A with **x**-axis pointing to the initial heading, and define $B = (x_f, y_f)$, φ_f are the destination and final heading; R is the turning radius. The centers of the left/right turn in Dubins motion are denoted by O_{AL}, O_{AR}, O_{BL}, and O_{BR}. The existences of motion types is shown in Table 1.

3.3 Steady State Solutions

Although the analytical relationship between glider motion configurations and control inputs can be found in the literature [41], we describe the development of an approximate semi-analytical solution to compute the steady state inputs of the glider motionsfor completeness. Let m_b denotes the ballast mass, r_{P1} denotes the linear position of the movable mass, and γ denotes the rotation angle of the movable mass. The rest of the definitions of parameters and coefficients appeared in this study are listed in Table 2.

Table 1 Situations of existing motion types

Motion types	Existance condition
LSL, RSR	(always exist)
LSR	$O_{AL}O_{BR} > 2R$
RSL	$O_{AR}O_{BL} > 2R$
LRL	$O_{AL}O_{BL} < 4R$
RLR	$O_{AR}O_{BR} < 4R$

Table 2 Definitions of variables appearing in glider motion

Title	Physical Significance
α, β	Angle of attack and slide
D, L	Drag and lift force components
$M_{DL1}, M_{DL2}, M_{DL3}$	Pitching moment components
K	Hydrodynamic coefficients
m	Vehicle heaviness
m_h	Vehicle hull mass
m_1, m_2, m_3	Added mass components
$\bar{m}$	Internal moving mass
g	Acceleration due to gravity
M_{f1}, M_{f2}, M_{f3}	Added mass terms
J_1, J_2, J_3	Added moment of inertia
$\Omega_1, \Omega_2, \Omega_3$	Roll/pitch/yaw rate
r_{P1}, r_{P2}, r_{P3}	Position of moving mass in body coordinates
ω_3	Turning angular velocity
Φ, θ, φ	Roll/pitch/yaw angle
p, q, r	Angular velocities in roll/pitch/yaw
V_1, V_2, V_3	Velocity components in body coordinates

The dynamic model of a glider modulated by a moving mass in the sawtooth path has been established and utilized. Graver and Leonard [42] provided the thorough derivation process of the 3-degrees-of-freedom (DOFs) model; Graver [43] provided the steady state solutions of the sawtooth motion in the vertical plane,

$$\alpha = \frac{1}{2}\frac{K_L}{K_D}\tan\xi \times\left(-1+\sqrt{1-4\frac{K_D}{K_L^2}\cot\xi(K_{D0}\cot\xi+K_{L0})}\right) \quad (4)$$

$$m_b = m-\bar{m}-m_h+\frac{V^2}{g}\left(-\sin\xi\left(K_{D0}+K_D\alpha^2\right) +\cos\xi\left(K_{L0}+K_L\alpha\right)\right) \quad (5)$$

$$r_{P1} = \frac{\left(m_3-m_1\right)V_1V_3+\left(K_{M0}+K_M\alpha\right)V^2}{\bar{m}g\cos\theta} -r_{P3}\tan\theta \quad (6)$$

where K_{L0}, K_L, K_{D0}, K_D, K_{M0}, and K_M are hydrodynamic coefficients.

However, the glider's equations of spiral motion are much more complicated because of the highly nonlinear and coupled terms triggered by the additional rotating mechanism. An approximate analytical solution for steady spiraling motion was derived by applying perturbation theory [37], where the first order solution is compared with the actual value, but the discrepancy between the approximate and actual values is distinct at low speed. A recursive algorithm based on the theoretical model has been used to compute the desired control input to produce a circular helix motion in [44], this algorithm uses the steady state model which neglects the rotational speed of the movable mass. Bhatta and Leonard [45] attempt to find numerical solutions to these equations that govern the spiral motion. In this study, an approximate semi-analytical solution method is applied, the derivation and verification process are sophisticated, this part of work has been summarized and introduced in [46].

Quite a few reasonable assumptions must be made to solve these equations:

Assumption 1 Neglect the coupled terms with minute value V_2, V_3, p, q, and r. It is because these variables are usually infinitesimal values at equilibrium, and can be neglected when coupled together.

Assumption 2 $V_1 = V$, $\cos\alpha = 1$, $\sin\alpha = V_3/V_1$, $\cos\beta = 1$, $\sin\beta = V_2/V_1$. Because V_2 and V_3 are always infinitesimal values compare to V_1.

Assumption 3 $\sin\alpha = \alpha$, $\sin\beta = \beta$. The first term of Taylor expansion is taken which has high degree of

approximation in this situation because both α and β are usually small values.

Therefore, the dynamic parameters appeared in the equations of spiral motion can be represented in the form of V_3:

$$\theta(V_3) = \xi + V_3/V_1 \tag{7}$$

$$m_b(V_3) = m - \bar{m} - m_h + \frac{-K_{D0}{V_1}^2 - K_D{V_3}^2 + K_{L0}V_1V_3 + K_L{V_3}^2}{g\sin\theta} \tag{8}$$

$$\phi(V_3) = -\varepsilon_1 \arctan\left[\frac{f_{\phi 2}{}^2 f_{\phi 3} - f_{\phi 1}\sqrt{f_{\phi 2}{}^2\left(f_{\phi 1}{}^2 + f_{\phi 2}{}^2 - f_{\phi 3}{}^2\right)}}{f_{\phi 1}f_{\phi 2}f_{\phi 3} + f_{\phi 2}\sqrt{f_{\phi 2}{}^2\left(f_{\phi 1}{}^2 + f_{\phi 2}{}^2 - f_{\phi 3}{}^2\right)}}\right] \tag{9}$$

$$p(V_3) = -\omega_3\cos\theta\tan\theta \tag{10}$$

$$q(V_3) = \omega_3\sin\phi\cos\theta \tag{11}$$

$$r(V_3) = \omega_3\cos\phi\cos\theta \tag{12}$$

$$V_2(V_3) = \frac{rV_1(m_h + \bar{m} + M_{f1}) - m_b g\cos\theta\sin\phi}{\varepsilon_2(K_\beta - K_{D0})V_1} \tag{13}$$

$$\gamma(V_3) = \arccos\frac{-f_{\gamma 1}f_{\gamma 4} - \sin\phi f_{\gamma 3}f_{\gamma 4} + \sqrt{\left(f_{\gamma 2} + \cos\phi f_{\gamma 3}\right)^2\left(f_\gamma - f_{\gamma 4}^2\right)}}{f_\gamma} \tag{14}$$

$$r_{P1}(V_3) = \frac{M_{DL2}\cos\beta + M_{DL1}\sin\beta + V_1V_3(M_{f3} - M_{f1}) - g\bar{m}\cos\gamma\sin\theta R_{mr}}{qV_1\bar{m} + g\bar{m}\cos\theta\cos\phi} \tag{15}$$

where $\varepsilon_1, \varepsilon_2$ are constant correction coefficients, $\omega_3 = V\cos\xi/R$, and

$$\begin{aligned}
f_{\phi 1} &= -K_{L0}{V_1}^2 - K_L V_1 V_3 - K_{D0}V_1V_3\\
f_{\phi 2} &= \bar{m}g\cos\theta\\
f_{\phi 3} &= \omega_3\cos\theta V_1(m_h + \bar{m} + M_{f1})\\
f_\gamma &= f_{\gamma 1}^2 + f_{\gamma 2}^2 + 2\sin\phi f_{\gamma 1}f_{\gamma 3}\\
&\quad +2\cos\phi f_{\gamma 2}f_{\gamma 3} + f_{\gamma 3}^2\\
f_{\gamma 1} &= rV_1\bar{m}R_{mr}\\
f_{\gamma 2} &= -qV_1\bar{m}R_{mr}\\
f_{\gamma 3} &= -g\cos\theta\bar{m}R_{mr}\\
f_{\gamma 4} &= K_{MR}V_1V_2 + K_p p{V_1}^2 - K_{M0}V_1V_2
\end{aligned}$$

where K_β, K_{MR}, and K_p, are hydrodynamic coefficients.

Finally, all of the dynamic parameters have been presented in the form of V_3. Substituting (7)–(15) back into the equations of spiral motion, the numerical solution of V_3 can be obtained. Substituting the value of V_3 back into Eqs. 7–15, every component in the equations of motion can be solved.

3.4 Energy Consumption Analysis

One significant characteristic and requirement of a glider's mission is to make the longest voyage with the minimal energy consumption. For a buoyancy driven glider with a pair of fixed wing and tail, whose attitude is modulated by an internal movable and rotatable mass, the energy can be generally divided into two parts: the energy used to actuate the mechanisms; and to the maintain the operation of the electronic system. In this part, the thorough energy consumption analysis of each subsystem is presented.

Typically, there are three mechanisms located inside an underwater glider: the buoyancy engine, the linear actuator, and the rotational actuator; the energy consumptions are denoted by E_b, E_l, and E_r, respectively. The energy consumption of the buoyancy engine E_b is correlated to the change of displacement and maximum operating depth D_{max}, is represented by:

$$E_b = \frac{2m_b}{\eta_b\rho}(n\rho g D_{\max} + \rho g D_m + nP_0) \tag{16}$$

where η_b is a constant value describing the total efficiency of the buoyancy engine; ρ is the density of ambient water; P_0 is the standard atmospheric pressure; n is the times of full-depth operation cycle, and D_m is the operating depth in the last cycle, which are denoted by:

$$n = \mathrm{In}\left(\frac{\sum_{i=1}^{3} S_i \tan\xi_i}{2D_{\max}}\right) \tag{17}$$

$$D_m = \mathrm{Re}\left(\frac{\sum_{i=1}^{3} S_i \tan\xi_i}{2D_{\max}}\right) \cdot D_{\max} \tag{18}$$

here, $\mathrm{In}(\cdot)$ and $\mathrm{Re}(\cdot)$ represents the value of integral part and remainder, respectively. S_i is the i-th length of projection of the 3D trajectory in the horizontal plane, ξ_i is the gliding path angle in i-th stage.

The energy consumption of the linear actuator E_l is related to the acceleration of the movable mass:

$$E_l = \frac{\bar{m}}{\eta_l} \int_{r_{P1s}}^{r_{P1e}} |\ddot{r}_x| dr_x \tag{19}$$

where r_{P1s} and r_{P1e} are the starting and end position of the moving mass, respectively. For conventional open-loop control, r_x can be represented by a function of time,

$$r_x = r_{P1}(1 - e^{-a_l r_{P1} t}) \tag{20}$$

where a_l is a constant value. Substitution (20) into Eq. 19, the energy consumption of the linear actuator is obtained:

$$E_l = \frac{2n+1}{\eta_l} \bar{m} {a_l}^2 r_{P1}^4 \tag{21}$$

Likewise, the expression of γ in the rotational actuator is

$$\gamma = -(\gamma_1 - \gamma_0) e^{-a_r(\gamma_1 - \gamma_0)t} + \gamma_1 \tag{22}$$

where γ_0 and γ_1 are the initial and final angle of rotation, respectively. Therefore the energy consumption of the rotational actuator is obtained:

$$E_r = \frac{1}{2\eta_r} a_r^2 (\gamma_1 - \gamma_0)^4 \tag{23}$$

where a_r is a constant value.

Distinguish from the energy consumption in the actuating of each mechanism, the maintenances of the electronic system will cost energy at a certain rate E_s, which can be represented by

$$E_s = \int_{t_0}^{t_f} a_s dt = \sum_{i=1}^{3} \frac{a_s S_i \sec\xi_i}{V} \tag{24}$$

where a_s is a constant value, t_0, and t_f are the initial and final time of motion, respectively.

Finally, the total energy consumption is the collectivity of the above subsystems:

$$E = E_b + E_l + E_s + \sum E_r \tag{25}$$

4 GA-based Path Planner

To obtain the optimal solution for the problem formulated in Section 3, an efficient optimization method should be applied. The optimal solution is concealed among the six feasible trajectories, and the total energy consumption function is highly nonlinear and coupled. Therefore, conventional linear optimization method has lost its favorable position in this situation. In this study, a multi-objective optimization based on GA is proposed in this section.

4.1 Integration of GA for 3D Dubins Path

The definition of parameters are listed in Table 3, and the pseudo code of the searching strategy for 3D Dubins path is illustrated in Table 4. The genetic algorithm, which is an iterative process, starts from a population of randomly generated candidate individuals. Each individual is represented in binary strings of

Table 3 Parameters appeared in the searching strategy

Parameters	Explanations
A, B	starting point and final destination
φ_A, φ_B	initial heading and final heading
D_{max}	maximum operating depth
$\mathbb{Z}$	Initial condition space $\mathbb{Z} = (A, B, \varphi_A, \varphi_B, D_{max})$
$\mathbb{R}$	boundarys of solution space
S_p	initial size of population
l_n, c_n	length and number of chromosome
P_c, P_m	the probability of crossover and mutant
n_i	iteration times
n_r	repetitive computation times

Table 4 Pseudo-code of the searching strategy

Pseudo-code	Explanations
for (i = 1:n_r)	repeat the calculation process
pop = round (rand (S_p, $l_n \cdot c_n$));	generate the initial binary population
for (j = 1:n_i)	one calculation process
Sol= decode((S_p, $\mathbb{R}$);	mapping into the solution space
Inp= solve (Sol);	solve the steady state equations
E6 = consp(Sol, Inp, $\mathbb{Z}$);	energy of all the existing situation
E = optimal(energy6)	choose the optimal energy and motion type
fitness = fit(E)	calculating the fitness of each individual
pop = selection(pop, fitness);	select the best solutions into next generation
pop = crossover(pop, P_c);	generate child individuals from mother ones
pop = mutation(pop, P_m);	alters one or more gene values
end	
end	

0s and 1s in the code space, which maps to the solution space. The components in the solution space are depend on the optimization situation, take one glider for example, the solution space is consisted of R, V, and ξ.

The analytical and approximate steady state solutions will be applied to obtain the control inputs, therefore, the energy consumption of each existing motion types can be calculated according to Section 3.4. The one with minimal energy consumption will be chosen as a candidate solution, which has a set of properties (its chromosomes or genotype) that can be mutated and altered.

The fitness of each individual in the population is evaluated through a measurement criteria of the objective function, an individual will possess a larger fitness value if the energy consumption is smaller. The fitter individuals are stochastically selected from the current population, and each individual's genome is modified (crossed and possibly randomly mutated) to form a new generation, which is prepared to use in the next iteration of the algorithm. The fitness proportionate selection (Roulette wheel selection) [47] method is applied to rate the fitness of each solution and preferentially select the best solutions:

$$p_i = \frac{f_i}{\sum_{j=1}^{pop} f_j} \tag{26}$$

where p_i is the probability of the individual of being selected, and f_i is the fitness of i-th individual in the population, which is determined by the energy consumption of each individual and the entire generation:

$$f_j = f \underset{j}{\in} \mathcal{F} \sum_{i=1}^{pop} evaluate(E_i) \tag{27}$$

where E_i is the energy consumption of i-th individual, $evaluate(E_i)$ is an evaluating process to every individual in the generation aims to establish the fitness function, and $\mathcal{F}$ is the fitness space.

The new individuals after the selection operator must be regenerated by crossover and mutation to maintain genetic diversity for the purpose of global searching in the solution space. Crossover is the exchange of genetic material between homologous chromosomes; while in mutation, any single gene has a certain probability to alter from its initial value (0 to 1, or 1 to 0).

In this way, newborn individuals are generated by a parent generation through the selection, crossover, and mutation process. The newborn generation will in turn become the parent generation in next iteration, this generational process will be repeated until a termination condition is reached. Considering the randomness of GA, the convergence of the solution should be verified through repetitive computation.

4.2 Rendezvous Planning with Optimized Final Heading

The proposed path planner of an underwater glider can be modified and applied to more complicated situations. For instance, a glider starts from a given initial point with an initial heading, the destination point is also specified while the final heading is flexible. On top of the GA optimization scheme integrated with 3D Dubins curve, the path planner will also involve one extra optimization module to optimize the final heading angle for the underwater glider. It is designed that the final heading angle can be flexible in a given range. In such situations, the choice of an appropriate final heading will be optimized based on the objective function.

4.3 Rendezvous Planning of Multiple Gliders

Versatile path planning system is of crucial importance to success and efficient rendezvous. This system need to capable of incorporating different factors influencing a given mission, like vehicles' dynamic constraints and initial conditions. The generic path planner can be extended to account for the case of path planning involving multiple underwater gliders. Each vehicle generates its trajectory as described above, but these trajectories will be optimized as an entire fleet based on the global objective. Various situations can be discussed in formation optimization: consider multiple underwater gliders start from given initial points with given initial headings and move to a given rendezvous point with an undetermined final heading; or the coordinate of rendezvous point is to be optimized with minimal energy consumption.

5 Case Study

In this section, we evaluate the performance and illustrate the capabilities of our methodology by applications to glider missions in simulating environments. Realistic glider rendezvous scenarios are discussed, including the docking of single glider and the rendezvous of multiple gliders.

Case 1 Path Planning for Docking of a Glider with Fixed Final Heading. This is the most common scenario where the glider is instructed to rendezvous with a stationary USV.

Case 2 Path Planning for Docking of a Glider with Optimized Final Heading. This considers the scenario where the glider is instructed to rendezvous with a intelligent dock with flexible final heading.

Case 3 Path Planning for Docking of a Glider in Short Range. This scenario aims to compare with Case 1, and indicate the difference in the optimal results caused by the discrepancy of planning range.

Then the generic GA-based path planner is extended to account for the case of planning trajectories for rendezvous of multiple underwater gliders. For simplicity, situations with two gliders are illustrated to demonstrate the capability of the proposed methodology.

Case 4 Path Planning for Rendezvous of Two Gliders with Optimized Final Heading. Two gliders are planned to move to the rendezvous point with flexible final heading, picked up by an USV or intercept with stationary platforms.

Case 5 Path Planning for Rendezvous of Two Gliders with Optimized Destination Position. This scheme is characterized by allowing the rendezvous position flexible to be optimized based on the objective function.

5.1 Parameter Setting

The model used in the simulation process is the Seawing [44] underwater glider, whose mechanical properties are: $m_h = 54.28/kg$, $\bar{m} = 11/kg$, $R_m = 0.014/m$, $I_{rb1} = 0.6/(kg \cdot m^2)$, $I_{rb2} = 15.27/(kg \cdot m^2)$, $I_{rb3} = 15.32/(kg \cdot m^2)$; and the hydrodynamic coefficients are listed in Table 5.

The coefficients appeared in Section 3.4 are: $\eta_b = 0.7$, $\eta_l = 0.85$, $\eta_r = 0.85$, $a_l = 0.1$, $a_r = 1$, $a_s = 1.5$. In the optimizing process, $n_i = 10$, $n_r = 100$, $P_c = 0.7$, $P_m = 0.05$, and the fitness function is

$$f_i = \begin{cases} (1 - E_i/E_{\min})^2 E_{\min}^2 & (E_i - E_{\min} < 1000) \\ 0 & (E_i - E_{\min} \geqslant 1000) \end{cases} \tag{28}$$

Table 5 Hydrodynamic coefficients of the Seawing glider

List of symbol	Value
Added mass terms M_A	diag[1.48, 49.58, 65.92]
Added inertia terms I_A	diag[0.53, 7.88, 10.18]
Added coupling terms C_A:	2.57, 3.61
Coefficients of drag force: K_{D0}, K_D	7.19, 386.29
Coefficients of lift force: K_{L0}, K_L	-0.36, 440.99
Coefficients of slide force: K_β	-115.65
Coefficients of M_{DL1}: K_{MR}, K_p	-58.27, -19.83
Coefficients of M_{DL2}: K_{M0}, K_M, K_q	0.28, -65.84, -205.64
Coefficients of M_{DL3}: K_{MY}, K_r	34.10, -389.30

where E_i is the energy consumption of i-th individual and E_{min} is the minimal value among them.

The optimized results are compared with the corresponding ones proposed in [38], where the vehicle travels at a nominal speed of $V = 0.4/(m \cdot s^{-1})$. According to [44], the optimal angle of attack is approximately $\alpha = \pm 7°$, which leading to an optimal gliding path angle of $\xi = \pm 13.6°$ by applying (5).

The boundary of turning radius is obtained with nominal travelling speed and gliding path angle, the relationship between the battery rotation angle γ and R is shown in [44]. The boundary chosen in this study is $R \in [50,\ 500]/m$, and the boundaries of velocity and diving path angle are $V \in [0.2,\ 0.8]/(m \cdot s^{-1})$ and $|\xi| \in [0.2,\ 1]/rad$, respectively. The maximum operating depth is $D_{max} = 100/m$.

5.2 Path Planning for a Single Glider

5.2.1 Case 1: Path Planning for Docking of a Glider with Fixed Final Heading

Problem Setup An underwater glider is moving from the initial position denoted by $A = (0, 0)$, and the initial heading is $\varphi_A = 0°$. An USV is used to pick up the vehicle, which located at $B_1 = (500, 700)$ with heading $\varphi_{B1} = 270°$. The GA-based path planner is applied to generate the trajectory with minimal energy consumption in the motion process. In this case, the initial size of population is $S_p = [10, 20, 50, 100, 200]$.

Figure 3 presents the monitoring of energy consumption and standard deviation of best individual in each iteration. The initial population of $S_p = 10$ and $S_p = 20$ is not converged within 10 iterations, which implies that the iteration time should be increased to guarantee the convergence. The curves with $S_p = 50$ and $S_p = 100$ perform well and the energy consumption converges fast and the standard deviation can be barely observed when $S_p = 200$. Therefore, larger initial populations will definitely have faster converge speed while the calculation amount increase rapidly at the same time.

Figure 4 presents the Dubins trajectory produced by GA path planner comparing to trajectory with nominal velocity and gliding path angle in Case 1. In the control group[38], the vehicle is travelling at a nominal velocity of $V_c = 0.4/(m \cdot s^{-1})$ and the gliding path

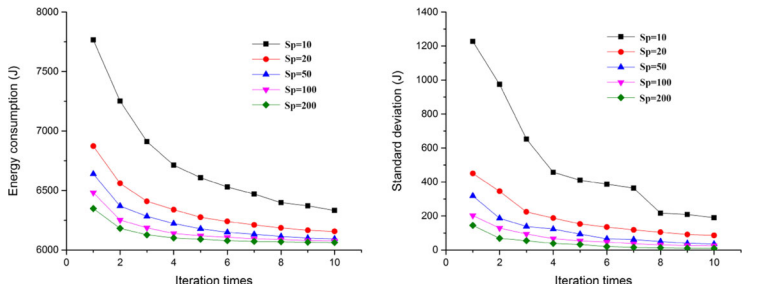

Fig. 3 Comparison of results produced by the GA path planner for a single glider (Case 1) with various population sizes

(a) Energy consumption (b) Standard deviation of best individuals

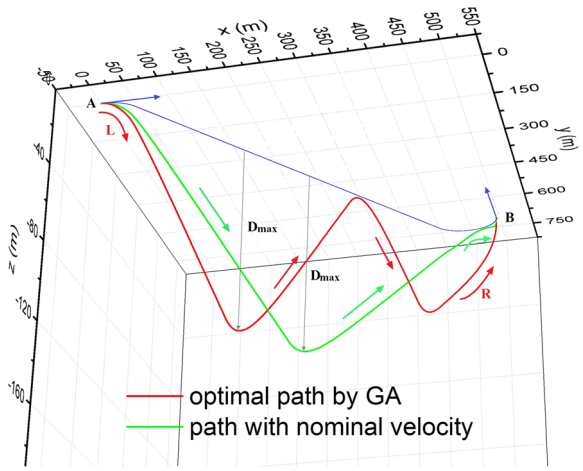

Fig. 4 Dubins trajectory produced by GA path planner versus trajectory with nominal velocity and gliding path angle (Case 1)

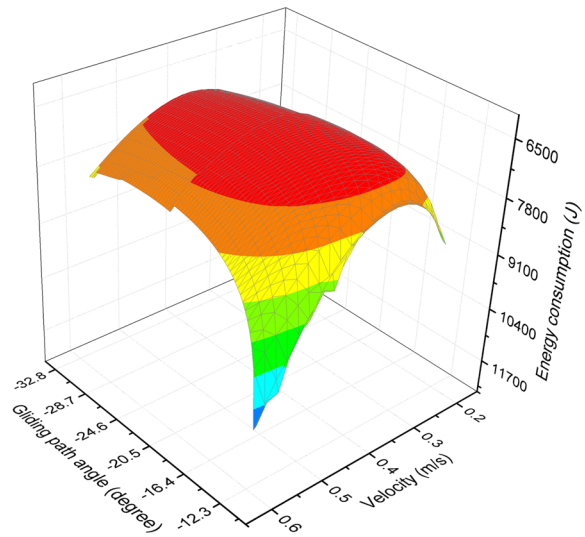

Fig. 5 Energy consumption vs. velocity and gliding path angle for $R = 50/m$ in Case 1

angle is $\xi_c = \pm 13.6°$, the optimal turning radius is at the minimal value: $R_c = 50/m$. Under this circumstance, the energy consumption of the motion process is $E_c = 7093/J$. In this study, the GA path planner is applied to optimize R, V, and ξ simultaneously. The optimal trajectory manners in LSR motion with one full-depth dive and a final regulating period. The results are $R_o = 50/m$, $V_o = 0.3824/(m \cdot s^{-1})$, and $\xi_o = \pm 20.91°$. The time duration of the process seems to be prolonged, which leads to the increasement of E_s; on the other hand, the energy consumptions in actuating mechanisms (E_l, E_r, and E_b) are reduced. As a consequence, the total energy consumption is reduced to $E_o = 6050/J$.

The effect of changing in velocity and gliding path angle on the total energy consumption when turning is specified has been studied, and the coupling relationship is presented in Fig. 5. The minimal energy consumption $E = 6050/J$ is located at $V = 0.38/(m \cdot s^{-1})$ and $\xi = \pm 20.9°$, which is consist with the optimal results obtained through the GA path planner. Much more energy consumption would be cost if the glider is in large velocity with small gliding path angle, which is a relatively bad situation in glider motion.

5.2.2 Case 2: Path Planning for Docking of a Glider with Optimized Final Heading

Problem Setup Case 2 considers a more complicate scenario where the glider is instructed to rendezvous with an intelligent dock. While the position of the dock is deterministic, its heading angle is flexible to be optimized. Let $A = (0, 0)$, $\varphi_A = 0°$, $B_2 = (500, 700)/m$, and φ_{B2} is flexible; comparing with Case 1, the solution space is extended to $\mathbb{R} = (R, V, \xi, \varphi_{B2})$.

The simulation results of average energy consumption and standard deviation is presented in Fig. 6, initial size of population is $S_p = [100, 200, 400]$. The number of chromosome in each individual increases when compared to Case 1, therefore, the initial size of population must be enlarged for the maintaining of convergence.

The simulation results converge to $R_o = 50/m$, $V_o = 0.3839/(m \cdot s^{-1})$, $\xi_o = \pm 20.91°$, $\varphi_{B2o} = 55.54°$, the trajectory starts with a left turn then moves straight to the destination as shown in Fig. 7. The optimal trajectory consists of a full-depth dive and a regulating period, while the corresponding path completes within one single period. However, the total energy consumption obtained through GA path planner is $E_o = 5475/J$, less than the energy cost in the nominal velocity path ($E_c = 6326/J$). The final turning stage can be barely observed in the figure, which suggests that the optimal trajectory in this scenario is a combination of beginning spiral motion and a sawtooth motion directly to the destination. Meanwhile, the translational velocity and gliding path angle are still motion configurations need to be optimized.

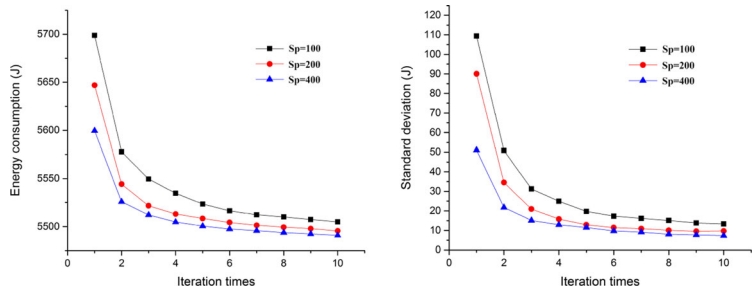

(a) Energy consumption (b) Standard deviation of best individuals

Fig. 6 Comparison of results produced by the GA path planner for a single glider (Case 2) with various population sizes

5.2.3 Case 3: Path Planning for Docking of a Glider in Short Range

Problem Setup In both Case 1 and Case 2, the optimal turning radiuses are converged to $R_o = 50/m$, which is the minimal value within the boundary, and consisted with the optimal results in planar Dubins problem. However, this consistency is not always readily available for 3D Dubins path of an underwater glider. Assume a glider starts from initial condition same as in Case 1, and the docking USV is located at $B_3 = (70, 60)/m$, which is a shorter distance compared to B_1, the final heading is $\varphi_{B3} = 60°$.

The optimization results converges to $R_o = 61.6/m$, $V_o = 0.3172/(m \cdot s^{-1})$, $\xi_o = \pm 25.89°$, as shown in Fig. 8. The optimal trajectory proposed in this study costs additional time duration and travels longer than the corresponding one, but the energy consumption indeed reduced from $E_c = 1189/J$ to $E_o = 811.5/J$, as shown in Fig. 9.

An interseting phenomenon is that the optimized turn radius does not converge to the minimal value as in the corresponding one. That is because the energy consumption in the rotation actuator E_r might be more significant than the buoyancy engine E_b and the electronic system E_s in short distance travelling situation.

5.3 Path Planning for Multiple Gliders

In the second set of simulations, another two case scenarios were designed to analyse the performance of this path planner for multiple gliders rendezvous. These case studies represent the scenario that two

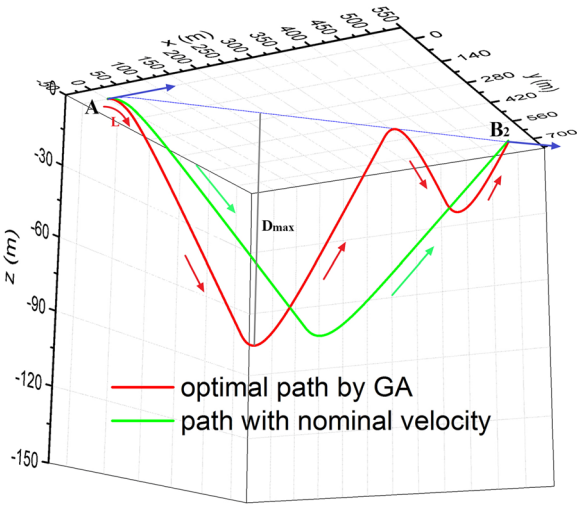

Fig. 7 Dubins trajectory produced by GA path planner versus trajectory with nominal velocity and gliding path angle (Case 2)

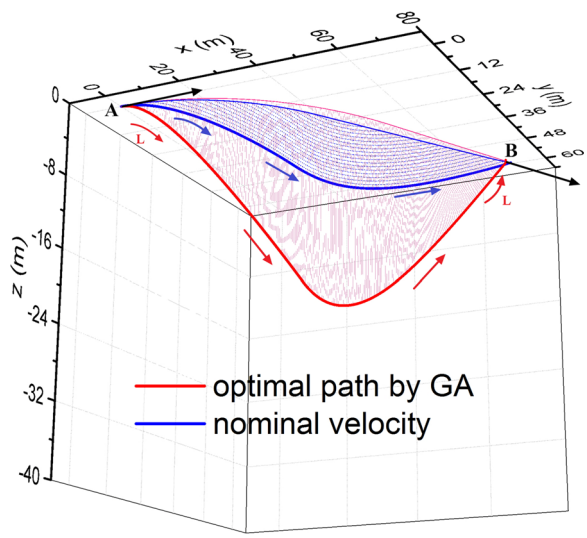

Fig. 8 Dubins trajectory produced by GA path planner ($R_o = 61.6/m$, $V_o = 0.3172/(m \cdot s^{-1})$, $\xi_o = \pm 25.89°$) versus trajectory with nominal velocity and gliding path angle($R_c = 50/m$, $V_c = 0.4/(m \cdot s^{-1})$, $\xi_c = \pm 13.6°$) for a single glider (Case 3)

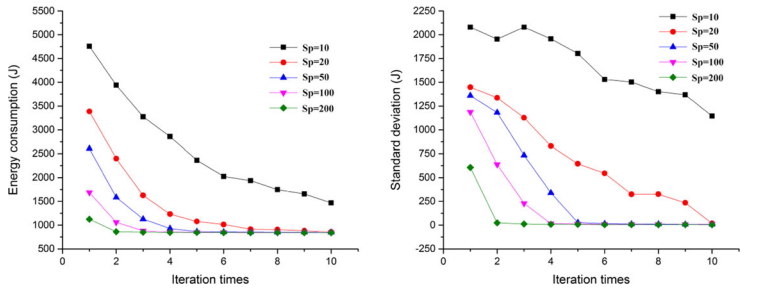

(a) Energy consumption (b) Standard deviation of best individuals

Fig. 9 Comparison of results produced by the GA path planner for a single glider (Case 3) with various population sizes of $S_p = [10, 20, 50, 100, 200]$

glider surfaces at the completion of the mission and would like to rendezvous with the USV for recovery. After surfacing, the glider transmits its location via satellite to the USV. The path planner system on the USV then identifies the optimal rendezvous point and calculates the trajectories that allow the two gliders to arrive at the rendezvous point with minimum amount of energy consumption as possible. In these two cases, path planner performance with both optimized final heading and optimized destination position, respectively, is studied.

5.3.1 Case 4: Path Planning for Rendezvous of Two Gliders with Optimized Final Heading

Problem Setup Assume that two gliders move from separate initial points $A_1 = (0, 0)$ and $A_2 = (150, 170)$, the initial headings are $\varphi_{A1} = 0°$ and $\varphi_{A2} = 120°$; the USV is stationary at $B = (100, 85)$. The path planning strategy is to generate the trajectories of gliders respectively, and to rendezvous at same destination with optimized heading. Therefore, the solution space is $\mathbb{R} = (R_1, V_1, \xi_1, R_2, V_2, \xi_2, \varphi_B)$.

Figure 10 presents the monitoring of energy consumption and standard deviation for two gliders in the simulation process, the size of population is enlarged to $S_p = 800$ due to the dimension of the solution space. The total energy consumption of the two gliders converges to $E_{tot} = 1833.2/J$. The optimal results are $R_{o1} = 50.37/m$, $V_{o1} = 0.3311/(m \cdot s^{-1})$, $\xi_{o1} = \pm 26.55°$, $R_{o2} = 55.54/m$, $V_{o2} = 0.3428/(m \cdot s^{-1})$, $\xi_{o2} = \pm 25.34°$ and $\varphi_{B_o} = 32.52°$, the trajectories are shown in Fig. 11. The path of A_1 performs in a LSR motion, and the turning radius is converged to the minimal value; while the path of A_2 is in LSL motion, and the turning radius is $R_{o2} = 55.54/m$. In addition, the path of A_1 is shorter than the path for A_2 due to the transient turning stage; while a large radian is necessary in the path for A_2 because point B locates in the second quadrant relative to A_2.

5.3.2 Case 5: Path Planning for Rendezvous of Two Gliders with Optimized Destination Position

Problem Setup Another application of the proposed strategy for multiple gliders is the optimization of

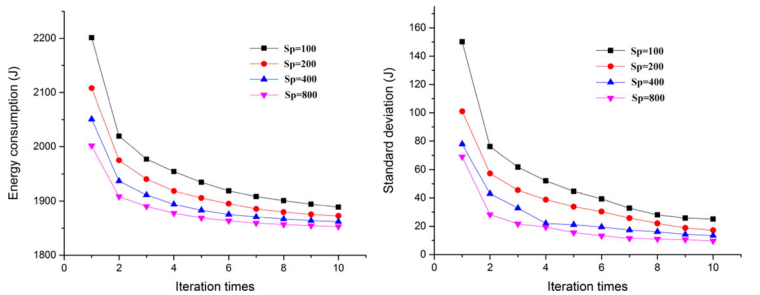

(a) Energy consumption (b) Standard deviation of best individuals

Fig. 10 Comparison of results produced by the GA path planner for two gliders (Case 4) with various population sizes of $S_p = [100, 200, 400, 800]$

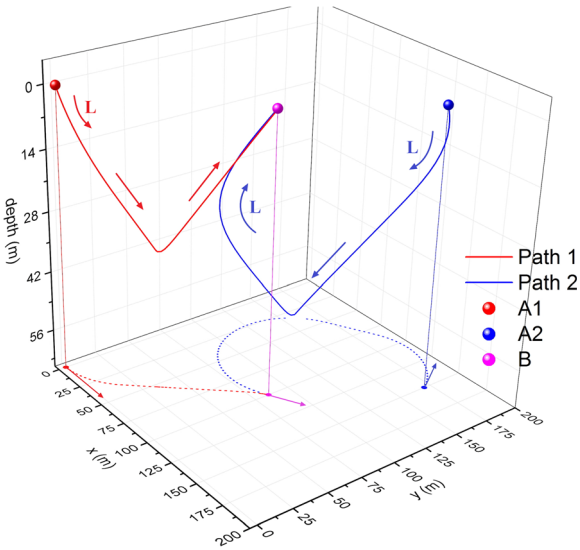

Fig. 11 Dubins trajectory produced by GA path planner for two gliders glider (Case 4) ($R_{o1} = 50.37/m, V_{o1} = 0.3311/(m \cdot s^{-1}), \xi_{o1} = \pm 26.55°, R_{o2} = 55.54/m, V_{o2} = 0.3428/(m \cdot s^{-1}), \xi_{o2} = \pm 25.34°$ and $\varphi_{B_o} = 32.52°$)

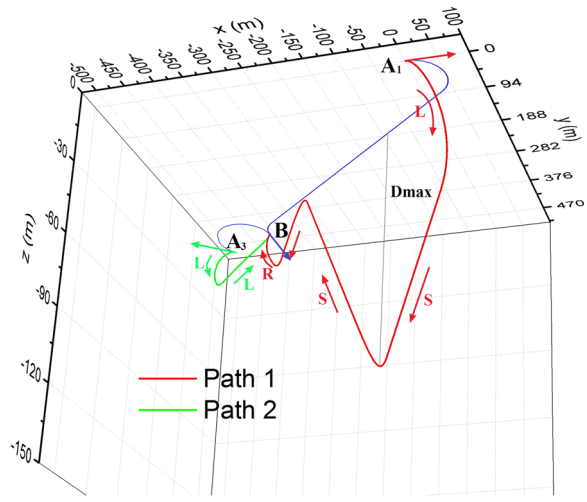

Fig. 13 Dubins trajectory produced by GA path planner for two gliders glider (Case 5) ($R_{o1} = 50/m, V_{o1} = 0.5480/(m \cdot s^{-1}), \xi_{o1} = \pm 29.06°, R_{o3} = 50/m, V_{o3} = 0.4254/(m \cdot s^{-1}), \xi_{o3} = \pm 18.09°, B_x = -410.6/m$, and $B_y = 451.6/m$)

the rendezvous position, which is a common scenario happens in the realistic situation. In this case study, the two gliders surfaces at $A_1 = (0, 0)$ and $A_3 = (-500, 500)$, with initial heading of $\varphi_{A1} = 0°$ and $\varphi_{A3} = 225°$, respectively, and the nominal final heading is $\varphi_B = 90°$.

Figure 12 presents the monitoring of energy consumption and standard deviation in the simulation process, the results didn't converge until the size of population is enlarged to $S_p = 1600$, because the additional coordinates of destination to be optimized lead to the expansion of solution space. The optimal results converge to $R_{o1} = 50/m, V_{o1} = 0.5480/(m \cdot s^{-1}), \xi_{o1} = \pm 29.06°, R_{o3} = 50/m, V_{o3} = 0.4254/(m \cdot s^{-1}), \xi_{o3} = \pm 18.09°, B_x = -410.6/m$, and $B_y = 451.6/m$. The two gliders move in LSR and LSL motion respectively, as shown in Fig. 13. The path of glider starts from A_1 travels longer than the one starts from A_3, so that the maximum operating depth is reached in Path 1.

In general, though only cases with two gliders have been considered in this study, the proposed strategy is able to solve the rendezvous problem for multiple gliders. The path planning process for more gliders can be considered as an amplification in calculation amount. However, the boundaries of the solution space can be narrowed through the simulation results of single glider cases, redundant calculations should be avoid in the optimization process.

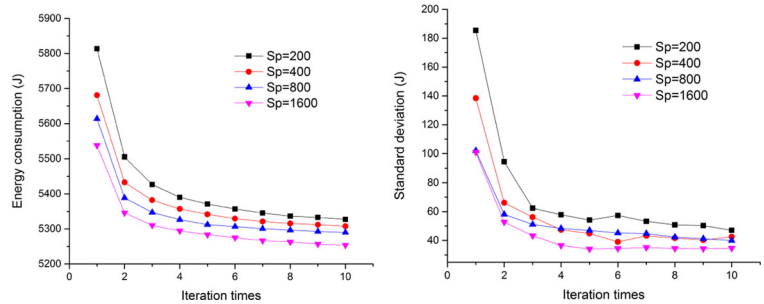

(a) Energy consumption (b) Standard deviation of best individuals

Fig. 12 Comparison of results produced by the GA path planner for two gliders (Case 5) with various population sizes of $S_p = [200, 400, 800, 1600]$

6 Conclusion and Future Work

This paper presents a novel path planning system that incorporates a modified 3D Dubins curve with GA to generate optimal trajectories for underwater gliders. Simulation tests have been performed to generate an optimal trajectory with minimum energy consumption for rendezvous of single and multiple underwater gliders in 3D environment. Based on the results of these tests, the GA-Dubins scheme is shown to be capable of is shown to be capable of finding a more optimized trajectory with less energy consumption compared to the nominal velocity Dubins path. The numerical case studies also suggest that the turning radius should be maintained at the minimal value when the distance is long; while the start and end point is within a short region, the radius might increases. This path planner is also integrated with an final heading angle selection scheme and an destination position selection scheme, respectively. The effectiveness and performance of this novel path planner is compared to the one with deterministic final heading and destination position. Experimental results demonstrate that path planner with optimal final heading and destination position obtains better solution that improves the performance of energy consumption for underwater gliders to complete the rendezvous mission.

The next stage in this work is to run the proposed techniques on a real glider operating in the ocean, and command it to follow the trajectory found by the path planner. The effective of the proposed techniques can be evaluated this way, as well as the accuracy of the glider motion model. One main limitation of the work completed so far is that no environmental noises have been considered, thus, the dynamics are simply evolving under a sequence of open-loop control instead of feedback control. A more sophisticated path planner, which incorporates the proposed method and feedback controller, is a valuable work in the future. Another extension of this work is to develop an on-line planning scheme [48–50] that can be incorporated into a glider's guidance system to allow it to regenerate the trajectory during the course of the mission.

Acknowledgments This study is supported by the National Natural Science Foundation of China (NSFC) (No. 51279107) and the Research Fund for Science and Technology Commission of Shanghai Municipality (STCSM) (No. 13dz1204600).

References

1. Stommel, H.: The SLOCUM mission. Oceanography **2**(1), 22–25 (1989)
2. Webb, D.C., Simonetti, P.J., Jones, C.P.: SLOCUM: An underwater glider propelled by environmental energy. IEEE J. Ocean. Eng. **26**(4), 447–452 (2001)
3. Sherman, J., Davis, R.E., Owens, W.B., Valdes, J.: The autonomous underwater glider Spray. IEEE J. Ocean. Eng. **26**(4), 437–446 (2001)
4. Eriksen, C.C., Osse, T.J., Light, R.D., Wen, T., Lehman, T.W., Sabin, P.L., Ballard, J.W., Chiodi, A.M.: Seaglider: A long-range autonomous underwater vehicle for oceanographic research. IEEE J. Ocean. Eng. **26**(4), 424–436 (2001)
5. Paley, D.A., Zhang, F., Leonard, N.E.: Cooperative control for ocean sampling: The glider coordinated control system. IEEE Trans. Control Syst. Technol. **16**(4), 735–744 (2008)
6. Xu, W., Liang, B., Li, C., Xu, Y.: Autonomous rendezvous and robotic capturing of non-cooperative target in space. Robotica **28**(05), 705–718 (2009)
7. Zeng, Z., Lammas, A., Sammut, K., He, F., Tang, Y., Ji, Q.: Path planning for rendezvous of multiple AUVs operating in a variable ocean. In: The 4th Annual IEEE International Conference on Cyber Technology in Automation, Control and Intelligent, pp. 451–456 (2014)
8. Giron-Sierra, J.M., Fernandez-Prisuelos, J., Andres-Toro, B.: Genetic control planning of autonomous underwater vehicles for rendezvous scenarios. WSEAS Trans. Syst. **5**(7), 1555–1563 (2006)
9. Zeng, Z., Lian, L., Sammut, K., He, F., Tang, Y., Lammas, A.: A survey on path planning for persistent autonomy of autonomous underwater vehicles. Ocean. Eng. **110**, 303–13 (2015)
10. Zamuda, A., Sosa, J.D.H.: Differential evolution and underwater glider path planning applied to the short-term opportunistic sampling of dynamic mesoscale ocean structures. Appl. Soft Comput. **24**, 95–108 (2014)
11. Smith, R.N., Schwager, M., Smith S.L., et al.: Persistent ocean monitoring with underwater gliders: Adapting sampling resolution. J. Field Rob. **28**(5), 714–741 (2011)
12. Codiga, D.L.: A Marine Autonomous Surface Craft for Long-Duration, Spatially Explicit, Multidisciplinary Water Column Sampling in Coastal and Estuarine Systems. J. Atmos. Ocean. Technol. **32**(3), 627–641 (2015)
13. Zhu, X., Yu, J., Wang, X.: Sampling path planning of underwater glider for optimal energy consumption. ROBOT **33**(3), 360–365 (2011)
14. Shuangshuang Fan, C.A.W.: Dynamics of underwater gliders in currents. Ocean. Eng. **84**, 249–258 (2014)
15. Dos Santos, R.R., Steffen Jr., V., Saramago, S.D.F.P.: Robot path planning in a constrained workspace by using optimal control techniques. Multibody Sys. Dyn. **19**(1–2), 159–177 (2008)
16. Crauser, A., Mehlhorn, K., Meyer, U., Sanders, P.: A parallelization of Dijkstra's shortest path algorithm, Mathematical Foundations of Computer Science, pp. 722–731. Springer, Berlin (1998)
17. Zeng, W., Church, R.L.: Finding shortest paths on real road networks: the case for A*. Int. J. Geogr. Inf. Sci. **23**, 531–543 (2009)

18. Ferguson, D., Stentz, A.: Using interpolation to improve path planning, The Field D* algorithm. J. F. Robot **23**, 79–101 (2006)
19. Staempfli, P., Jaermann, T., Crelier, G.R., Kollias, S., Valavanis, A., Boesiger, P.: Resolving fiber crossing using advanced fast marching tractography based on diffusion tensor imaging. Neuroimage **30**, 110–20 (2006)
20. Khatib, O.: Real-Time Obstacle avoidance for manipulators and mobile robots. Int. J. Rob. Res **5**, 90–98 (1986)
21. LaValle, S.M., Kuffner, Jr, J.J.: Rapidly-Exploring Random Trees: Progress and Prospects
22. Zeng, Z., Lammas, A., Sammut, K., He, F., Tang, Y.: Shell space decomposition based path planning for AUVs operating in a variable environment. Ocean. Eng. **91**, 181–195 (2014)
23. Alvarez, A., Caiti, A., Onken, R.: Evolutionary path planning for autonomous underwater vehicles in a variable ocean. IEEE J. Ocean. Eng **29**, 418–429 (2004)
24. Nikolos, I.K., Valavanis, K.P., Tsourveloudis, N.C., Kostaras, A.N.: Evolutionary algorithm based offline/online path planner for UAV navigation. IEEE Trans. Syst. Man. Cybern. B. Cybern. **33**, 898–912 (2003)
25. Besada-Portas, E., Lopez-Orozco, J.A., de la Torre, L., de la Cruz, J.M.: Remote Control Laboratory Using EJS Applets and TwinCAT Programmable Logic Controllers. IEEE Trans. Educ. **56**, 156–164 (2013)
26. Roberge, V., Tarbouchi, M., Labonte, G.: Comparison of parallel genetic algorithm and particle swarm optimization for Real-Time UAV path planning. IEEE Trans. Ind. Informatics **9**, 132–141 (2013)
27. Furtuna, A.A., Balkcom, D.J.: Generalizing Dubins Curves: Minimum-time Sequences of Body-fixed Rotations and Translations in the Plane. Int. J. Rob. Res. **29**, 703–726 (2010)
28. Dubins, L.: On curves of minimal length with a constraint on average curvature, and with prescribed initial and terminal positions and tangents. Am. J. Math. **79**, 497–516 (1957)
29. Isaiah, P., Shima, T.: Motion planning algorithms for the Dubins Travelling Salesperson Problem. Automatica **53**, 247–255 (2015)
30. Jurdjevic, V.: The Delauney-Dubins Problem, Geometric Control Theory and Sub-Riemannian Geometry, pp. 219–239. Springer International Publishing, Switzerland (2014)
31. Techy, L., Woolsey, C.A.: Minimum-time path planning for unmanned aerial vehicles in steady uniform winds. J. Guid. Control. Dyn. **32**(6), 1736–1746 (2009)
32. Shanmugavel, M. et al.: 3D Dubins sets based coordinated path planning for swarm of UAVs. In: AIAA Guidance, Navigation, and Control Conference and Exhibit, Keystone, CO (2006)
33. Myung, H., Kuffner, J., Kanade, T.: Efficient two-phase 3d motion planning for small fixed-wing uavs, Robotics and Automation, 2007 IEEE International Conference on. IEEE (2007)
34. Lin, Y., Saripalli, S.: Path planning using 3D dubins curve for unmanned aerial vehicles, Unmanned Aircraft Systems (ICUAS), 2014 International Conference on. IEEE (2014)
35. Zhu, D., Huang, H., Yang, S.X.: Dynamic task assignment and path planning of multi-AUV system based on an improved self-organizing map and velocity synthesis method in three-dimensional underwater workspace. IEEE Trans. Cybern. **43**(2), 504–514 (2013)
36. Xiang, C., Zhu, D., Simon, X.Y.: Multi-AUV target searching under ocean current based on PPSO and velocity synthesis algorithm. Underw. Technol. **33**(1), 31–39 (2015)
37. Mahmoudian, N., Geisbert, J., Woolsey, C.: Approximate analytical turning conditions for underwater gliders: Implications for motion control and path planning. IEEE J. Ocean. Eng. **35**(1), 131–143 (2010)
38. Mahmoudian, N., Geisert, J., Woolsey, C.: Dynamics and Control of Underwater Gliders I: Steady Motions. Technical Report, Virginia Polytechnic Institute and State University (2009)
39. Kostov, V.P., Degtiariova-Kostova, E.V.: The planar motion with bounded derivative of the curvature and its suboptimal paths. Acta Math. Univ. Comenianae **64**(2), 185–226 (1995)
40. Boissonnat, J.-D., Crzo, A., Leblond, J.: Shortest paths of bounded curvature in the plane. Springer, Berlin (1993)
41. Mahmoudian, N., Woolsey, C., Geisbert, J.: Steady turns and optimal paths for underwater gliders, Hilton Head, SC (2007)
42. Graver, J.G., Leonard, N.E.: Underwater glider dynamics and control. 12th international symposium on unmanned untethered submersible technology, 1710–1742 (2001)
43. Graver, J.G.: Underwater gliders: Dynamics, control and design[D]. Princeton University, Princeton (2005)
44. Zhang, S., Zhang, A., et al.: Y. J. Spiraling motion of underwater gliders: Modeling, analysis, and experimental results. Ocean Eng. **60**, 1–13 (2013)
45. Bhatta, P., Leonard, N.E.: Nonlinear gliding stability and control for vehicles with hydrodynamic forcing. Automatica **44**, 1240–1250 (2008)
46. Cao, J., Cao, J., Zeng, Z., Lian, L.: Dynamics and Approximate Semi-analytical Solution of an Underwater Glider in Spiral Motion, Indian Journal of Geo-Marine Sciences, (accepted)
47. Carlson, S.E.: Genetic algorithm attributes for component selection. Res. Eng. Des **8**, 33–51 (1996)
48. Zeng, Z., Sammut, K., Lammas, A., He, F., Tang, Y.: Efficient Path Re-planning for AUVs Operating in Spatiotemporal Currents J Intell. Robot Syst (2014)
49. Yazdani, A.M., Sammut, K., Lammas, A., Tang, Y. (eds.): Real-time quasi-optimal trajectory planning for autonomous underwater docking. In: IEEE International Symposium on Robotics and Intelligent Sensors (IRIS) (2015)
50. Zadeh, S.M., Powers, D.M., Yazdani, A.M.: Development of an Autonomous Reactive Mission Scheduling and Path Planning (ARMSP) Architecture Using Evolutionary Algorithms for AUV Operation in a Sever Ocean Environment (2016). arXiv preprint arXiv:160501824

Junliang Cao was born in China in 1989. He received his B.S. degree in mechanical engineering in 2011, from University of Michigan - Shanghai Jiao Tong University Joint Institute (UMJI). He is currently a Ph.D candidate in the State Key Laboratory of Ocean Engineering, Shanghai Jiao Tong University (SJTU). His Ph.D works are focused on dynamics, automatic control, and path planning of underwater vehicles. He is an IEEE student member, and the chair of the Ocean Engineering Society (OES) student chapter in China.

Junjun Cao is a Ph.D. student in the Ship & Ocean Engineering Department at the Shanghai Jiao Tong University. He received the B.S. and M.S. degree in Ship Architecture and Ocean Engineering Department from the Harbin Engineering University, in 2011 and 2014, respectively. His research interests include design and analysis of underwater glider systems, hydrodynamic analysis and path planning of underwater vehicles. His Ph.D. research focused on path planning and adaptive sampling of multi-gliders operating in variable oceans.

Zheng Zeng completed his Ph.D. research at the Centre for Maritime Engineering, Control and Imaging in Flinders University, Australia and now a research fellow at Shanghai Jiao Tong University, China. His particular areas of research specialization are concerned with Autonomous Marine Vehicles (AMVs) including optimal guidance, navigation, and control systems. He is a reviewer for multiple international scientific journals, he is a committee member for IEEE-OES/MTS OCEANS'16Shanghai conference and he currently serves as the secretary for IEEE-OES Shanghai Section.

Baoheng Yao is an associate professor of Shanghai Jiao Tong University in China. He received his B.S. degree in mechanical engineering from Fuxin Mining Institute in 1994, and Ph.D degree in mechatronics engineering from Shanghai Jiao Tong University in 2005. His areas of interests include nonlinear dynamics, fluid mechanics and subsea technology.

Lian Lian received her Bachelor's degree and Master's degree in Naval Architecture & Ocean Engineering, and the PhD Degree in Technology Management from Shanghai Jiao Tong University. She has become a full professor of Shanghai Jiao Tong University since 1998, and served as a member of expert group of National Hi-Tech Program (863 Program) from 1999–2011, a member of Member of Expert Group of National Science Foundation of China from 2008-2011. Now she is the Vice Dean of Institute of Oceanology, Shanghai Jiao Tong University, IEEE/OES Shanghai Chapter Chair and the General Chair of OCEANS'16 Shanghai. Her research mainly focuses on underwater vehicles, marine observation.